Proceedings of the ASME 2014 Pressure Vessels & Piping Conference
PVP2014
July 20-24, 2014, Anaheim, California, USA

PVP2014-28449

BUCKLING AND LATERAL PRESSURES IN SPIRAL WOUND GASKETS

Hocine Attoui **Abdel-Hakim Bouzid** **Jerry A. Waterland**

ABSTRACT

The buckling of spiral wound gaskets (SWGs) causes turbulence of the fluid flow inside flanges and may result in leakage failure over time due to the unwinding of the spirals. A few limited studies on the lateral forces generated by axial compression of the gasket sealing element which cause this phenomenon are available in the literature. The lateral forces are generated during initial tightening and are not distributed uniformly in the circumferential direction. Hence there is an introduction of concentrated forces in small areas.

The non-uniform gasket contact stress caused by the tightening sequence makes the problem more complex. It is suggested to study experimentally the buckling of spiral wound gaskets by developing a special test bench designed for this purpose. This test bench is able to measure the lateral loads and winding inward displacement during the tightening process. The experimental results are to be compared to those obtained by numerical FE simulation for the purpose of extrapolating for other size gaskets.

INTRODUCTION

In general, industrial installations that use pressurized equipment are routinely subjected to leakage failure and the unintended escape of fluids. When these leaks exceed acceptable limits, they can cause accidents, shut downs of units, environmental damage, and loss of revenue. Gaskets are used in the mechanical components of these industrial installations to contain these fluids and prevent fluid loss. The reliability of this equipment is evaluated by their capacity of confining pressure, i.e. to prevent the fluid from escaping towards the outside of the equipment. A spiral wound gasket (SWG), is composed of metal windings and a filler made of a softer material, an outer ring to limit the compression and an inner ring to reduce buckling. The most critical part is the sealing element. There is limited research on spiral wound gasket behavior and only few papers treat their buckling [1,2].

The SW gasket is compressed by clamping the bolts using a tightening procedure which exerts a non-uniformly distributed load on the sealing element or the windings. Referring to Fig. 1, the axial compression of the windings transfers the load to the inner and outer rings, through the contact areas, and introduces radial contact pressures that can cause buckling. The quality of the sealing performance of the gasket depends on the values of these radial contact stresses.

The axial compression increases with the clamping bolts and causes deformation of the windings towards the inside of the pipe. The knowledge of the relationship between axial load compression, generated contact pressure and the nature of winding deformation is the key solution to solve the buckling problem and improve the sealing performance [3].

This paper evaluates the buckling issue of the outer ring and inward buckling of the windings by indirect measurements of the radial contact pressure or lateral pressure generated during compression. Therefore, the characteristics of a SW gasket are obtained by a numerical-experimental procedure. Then the results are evaluated and compared to the ones obtained by numerical simulation.

NOMENCLATURE

a	outer radius of packing or ring
A	cross section area of ring
C_1, C_2, C_3	coefficients
c	autofrettage radius
D_n	lateral displacement of windings
E	Young's modulus
G	shear modulus

h	ring thickness
I_x	2nd moment of inertia of the section along the x axis
I_z	2nd moment of inertia of the section along the z axis
I_p	polar moment of inertia of the section
J	torsion constant
n	buckling mode number
P_A	Autofrettage pressure
P_c	Contact pressure
P_{cr}	Critical buckling pressure
r	Radial position of strain gage on ring
R_e	Outer radius of the ring
R_{eg}	Outer radius of the sealing element
R_p	Distance from the center to the point of consideration
S_g	Gasket compressive stress
S_y	Yield stress of steel
t	ring width
U_y	crushing or axial movement of the seal
Y_e	R_e/R_{eg}
σ_{cr}	critical buckling stress
α	GJ/EI_z
β	I_p/Aa^2
γ	$P a^3/EI_x$
λ	$P a^3/EI_z$
κ	Aa^2/I_x
ν_e	Poisson's ratio

BACKGROUND

Few researchers have proposed analytical models supported by experimental studies to determine the lateral pressure coefficient and the critical buckling load for different type of SW gaskets [4]. In most existing buckling studies of SW gaskets the research is focused on the outer ring without considering the windings or the filler. Timoshenko [5] presented the theoretical background of buckling curved beams, rings and shells. Tein Wah [6] studied the buckling of rings and separated the buckling modes by; in plane of the ring, and the one that happens outside of the plane. J. E. Goldberg [7] studied the lateral buckling of circular section by double-tree rings and considered the case of a closed ring. The formulas presented are valid only for single sections or double symmetry. Thomas [8] dedicated a complete thesis on the buckling in the plane and out of plane of thick rings subjected to hydrostatic radial pressure. He compared different theories using several ring sizes with rectangular cross sections. He compared the theories of thin rings and thick rings to predict buckling, and proved the two theories agree with each other within 10% difference for diameter to thickness ratio D/t over 20. He also concluded the theory of thick rings is inaccurate for ratio less than 5.

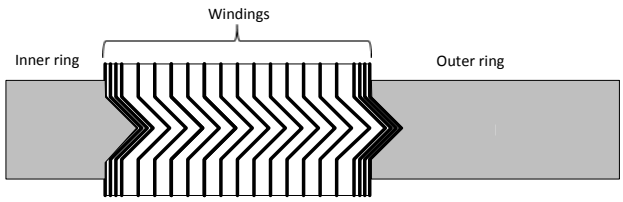

Figure 1: Spiral wound gasket with outer ring

Teng and Lucas [9] developed a closed-form solution based on the thin-walled member theory of the out-of-plane buckling of thin ring with an open cross section. In their developed model a simplified mathematical expression is obtained for the buckling resistance of an angle section ring loaded and supported at its inner edge. They confirmed the accuracy of their model when applied to a closed section by comparison with numerical FE analysis. Boresi [10] made an effort to explain the buckling of the flanges using the energy method. Weeks [11] studied the critical buckling loads of a pressurized toroidal ring under a uniformly distributed line load, with finite shear stiffness, extensional stiffness, and the appropriate contributions from the internal pressure. In his study, the equations governing both in-plane and out-of -plane buckling behavior of the ring for the three directions of loading have been derived and solved, and simple buckling formulas are given.

In the present study, the models presented by Tein and Wah, and that of Tang and Lucas are used to study the buckling of the SW gaskets. In parallel, 2D axisymmetric numerical simulation is used to support the two models. Finally, an experimental investigation on SW gaskets with outer rings and no inner rings was conducted on an NPS 4 class 900 weld neck bolted joint to validate the model used.

EXPERIMENTAL ASSEMBLY

A test apparatus as is illustrated in Fig. 2 is specifically developed to conduct experimental buckling investigations of SW gaskets. The gasket is made of preformed metallic v-shaped strip and a soft filler material wound together under pressure, with an outer guide ring. The latter has the function of centering the gasket in the flanges and gives the sealing elements additional resistance against line pressure while limiting gasket displacement due to excessive bolt torque.

The test fixture consists of a pair of NPS 4 class 900 welding neck flanges; the bottom flange is supported by a stand anchored directly to the floor as shown in Fig. 2. Several measuring devices are installed in the apparatus and connected to a computer through a data acquisition system. All 8 bolts are instrumented to measure the bolt force by means of special circular bolt strain gages used in quarter bridges and calibrated on an MTS servo-hydraulic tensile machine. Three LVDT's placed at 120 degrees on the lower flange are used to measure

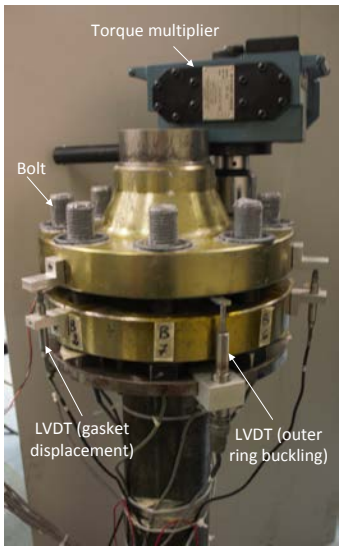

Figure 2 Instrumented NPS 4 class 900 bolted joint

gasket displacement due to compression. A special device was designed and fabricated in the laboratory to measure the radial displacement of the gasket due to compression and any inward buckling displacement of the windings. The inward buckling measuring device is shown in Fig. 3. It is composed of nine full bridge strain gaged instrumented beams which are equispaced and held secure to a circular base that can be introduced inside the flange and fixed at its weld neck inner diameter. The device position is adjusted so that the beam rod extremities come in permanent contact with the first metal winding at inner circumference of the gasket. Any radial movement of the windings will cause flexion of the beams which is detected through the full bridge strain gages. A micrometer is used to calibrate the nine beam sensors prior to testing. An additional three LVDT's are used to measure any axial movement of the outer ring to detect any out-of plane buckling produced by the lateral load. Extension beams are clamped to the outer ring to transmit the movement to the LVDT placed at the flange outer periphery shown in Fig. 3. A strain gage is placed at an

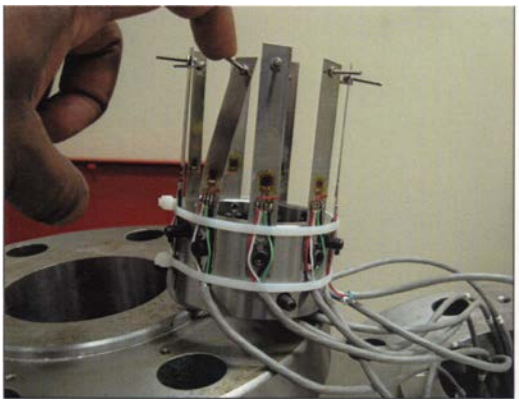

Figure 3: Inward radial displacement sensor

arbitrary radial distance of 88 mm on the surface of each outer ring to measure the hoop strain from which the radial load can be deduced.

Bolt initial tightening is performed using a digital power torque multiplier device capable of transmitting up to 1200 lb.ft which can produce a gasket stress of 300 MPa. The criss-cross pattern is used to tighten the bolts. All instruments are connected to a data acquisition system and the data is transferred to a computer that runs with LabView software.

NUMERICAL FINITE ELEMENT SIMULATION

A 2D axisymmetric model of the configuration of the SW gasket is simulated numerically using the general purpose finite element ANSYS software [12]. The model mesh shown in Fig. 4 uses 8-nodes axisymmetric plane elements to model the windings, the graphite filler and the outer ring. This model is used to study the behavior of the interaction between the sealing element and the ring when the gasket is subjected to a compressive stress to produce an axial displacement.

The SW gasket of NPS 4 class 900 is made of stainless steel. The sealing element made of graphite and metal winding is not modeled as a gasket equivalent model [13]. In fact 25 metal strip windings and 15 graphite windings are modeled [14]. Contact and target elements are used to simulate the relative movement at the contact interface between graphite and steel windings. The displacement of the bottom of the sealing element is blocked in the axial direction while the upper surface is subjected to a pressure to simulate the gasket compressive stress as a result of bolt tightening.

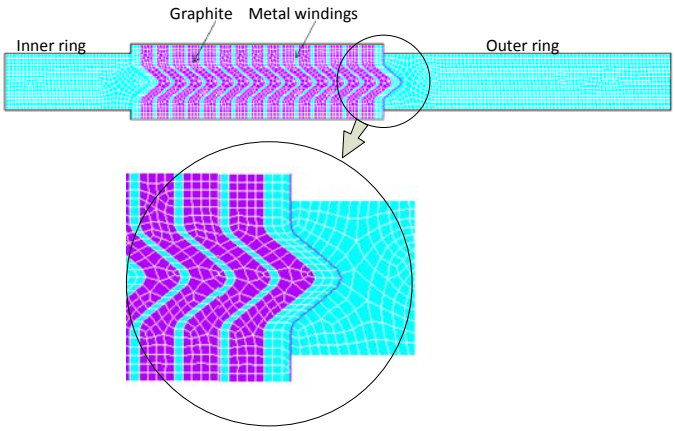

Figure 4 FE mesh model of a SW gasket

THEORETICAL BUCKLING MODELS

Two models are used to obtain the buckling load of the spiral wound gasket outer ring; the model of Tein Wah and the model of Tang and Lucas. The ring used has a rectangular cross section the dimensions. Wah has developed two equations that describe the buckling modes of a ring subjected to a radial distributed force. The first equation describes the in-plane buckling and the second equation describes the out-of-plane

buckling such that:

$$\gamma^2 - \gamma\left(\kappa + n^2\right) + \kappa\left(n^2 - 1\right) = 0 \quad (1)$$

$$\beta^2 - \beta\left(n^2 + \alpha + \frac{\alpha}{\beta} + \frac{1}{\beta n^2}\right) + \frac{\alpha\left(n^2-1\right)^2}{\beta n^2} = 0 \quad (2)$$

The first equation gives the critical first load of interest when n=2

$$P_{cr} = \frac{3EI_x}{a^3} \quad (3)$$

The second equation gives the out-of-plane critical buckling

$$P_{cr} = \frac{9\alpha}{1+4\alpha}\frac{EI_z}{a^3} \quad (4)$$

Tang and Lucas give the solution for the out-of-plane buckling in terms of the critical stress or the load as:

$$\sigma_{cr} = \frac{I_z}{A_s r_0^2}\left[\frac{\lambda\left(1-C_3\right)^2 + C_1 C_3\left(1-\lambda\right)^2}{C_3 - C_2}\right]E \quad (5)$$

$$P_{cr} = \frac{\sigma_{cr} A_s}{hR_p} \quad (6)$$

C_1, C_2 and C_3 are constants given by

$$C_1 = \frac{GJ}{EI_z} \qquad C_2 = \frac{tr_c}{r_0^2} \quad (7)$$

$$C_3 = C_2\left[1 + \sqrt{\left(1 - \frac{1}{C_2}\right)^2 + \frac{C_1}{\lambda C_2}\left(1-\lambda\right)^2}\right] \quad (8)$$

$$\lambda = \frac{t}{r_c} \qquad r_0^2 = \left[\frac{I_p}{A_s}\right] + r_c^2 + y_c^2 \quad (9)$$

Where r_c and y_c are the ring radius and axial distance of centroid. Here y_c is equal to zero. The second moments of area I_x and I_z, the polar moment of area and the torsional constant are given as follows:

$$I_x = \frac{ht^3}{12}$$
$$I_z = \frac{th^3}{12}$$
$$I_p = \frac{ht^3}{12} + \frac{th^3}{12} \quad (10)$$
$$J = \frac{th^3}{3}\left[1 - \frac{192}{\pi^5}\frac{h}{t}\tanh\frac{\pi t}{2h}\right]$$

The critical in-plane buckling load of the windings placed concentric without graphite is given by the following equation.

$$P_{cr} = \frac{3\left(n^2-1\right)}{h}\sum_{i=1}^{m}\frac{E_i I_{X_i}}{r_i^3} \quad (11)$$

Where i is the stainless steel winding number and m is the number of steel windings considered for the inward buckling for the SW gasket. Only the first few windings that do not have graphite could be considered.

CALCULATING THE RADIAL CONTACT PRESSURE

Once the experimental measurement of the hoop deformation at the surface of the outer ring is known, Lamé equations for thick-walled cylinder [15] are used for calculating the lateral pressure P_c when the ring is in the elastic domain such that:

$$p_c = \frac{E\left(Y_e^2 - 1\right)}{\left(1-\nu_e\right) + \left(1+\nu_e\right)\frac{R_e^2}{r^2}}\varepsilon_\theta \quad (12)$$

If the ring is plastically deformed, the theory of autofrettaged cylinder is used to determine the lateral pressure [16,17]. The pressure required to produce plasticity till a radius c is given by:

$$P_c = S_y\left[\frac{1}{2}\left(\frac{Y_e^2 - 1}{Y_e^2}\right) - \ln\frac{R_{eg}}{c}\right] \quad (13)$$

RESULTS AND DISCUSION

The spiral wound gasket consists of two main parts which are the outer ring and the sealing element. Analysis of the lateral pressure generated by compression shows that

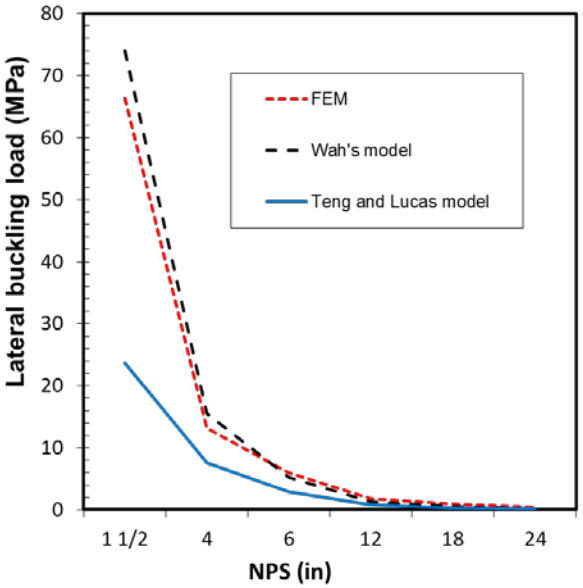

Figure 5: Buckling of inner ring of class 900 SW gaskets: Analytical and numerical FE results

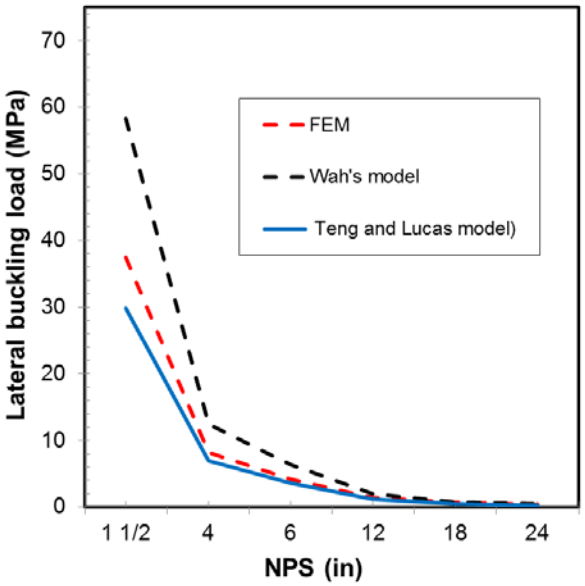

Figure 6: Buckling of outer ring of class 900 SW gaskets:

compression can cause buckling of the different elements of the SW gasket. In the presence of the inner and outer rings, the buckling loads for SW class 900 lb, as an example, are given in Figs. 5 and 6. The results of the two analytical models are compared to those obtained by FEM.

For the inner ring, as shown in Fig. 5, the Wah model that predicts in-plane buckling using Eq.(3) gives results that are close to the FE counterparts. The difference is small at the small sizes gaskets; 11% for NPS 1½ and 55% for NPS 24. The Teng and Lucas model predicts lower loads and the difference is higher but rather constant for all sizes (about 55%). A buckling lateral pressure of 20 MPa is predicted for an

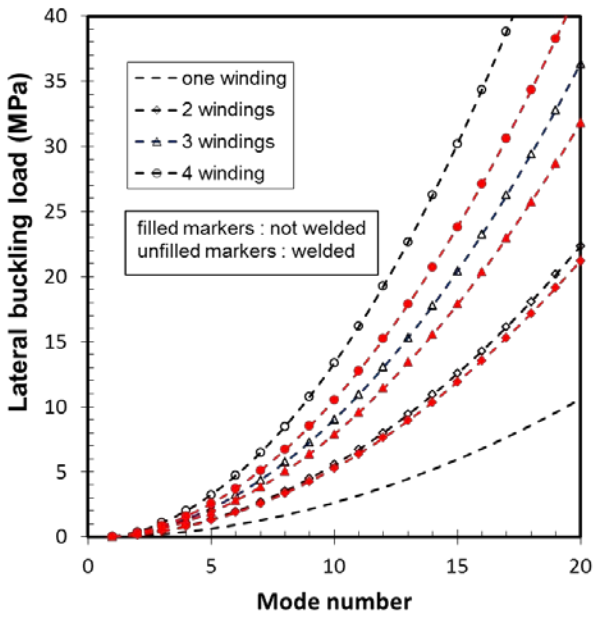

Figure 7: Relationship between load and windings

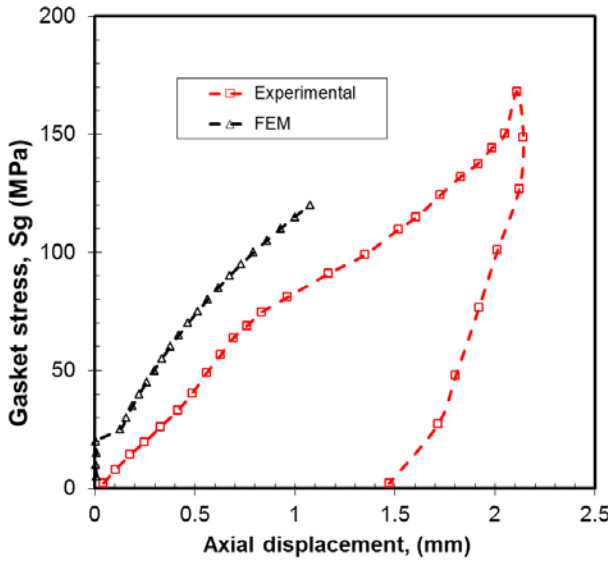

Figure 8: Relationship between compression Sg and NPS 4 class 900 inner ring.

For the outer ring, predictions of the out-of-plane buckling are given in Fig. 6. The results show that Teng and Lucas are close to the FE results. The maximum difference between them is 31%. Way model predicts higher loads and the maximum difference is 55% obtained at the lower size. The predicted out-of-plane buckling of the inner ring of the NPS 4 class 900 SW gasket used in the test rig is about 7 MPa. In general, the buckling loads of the outer rings are smaller than those of the inner rings; this is why the out-of-plane deformation of outer rings is reported in the litterature more often than inner ring contrepart.

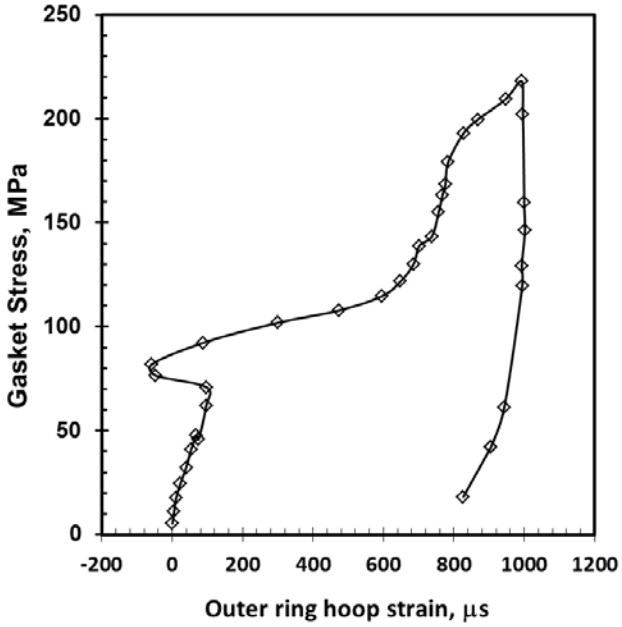

Figure 9: Measured outer ring Hoop strain

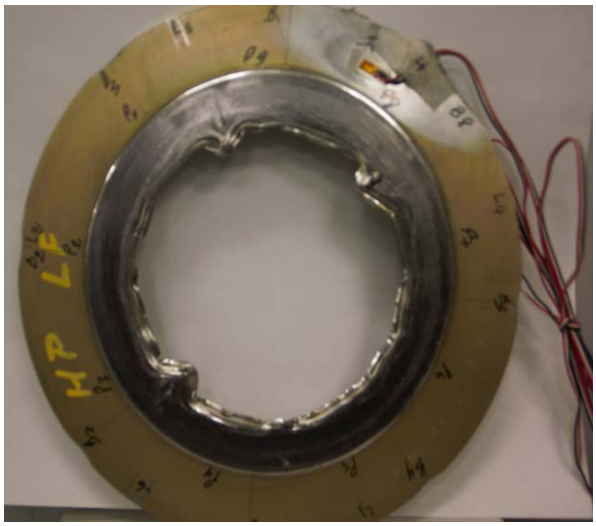

Figure 10: SW gasket showing buckled windings

The metal windings of the sealing element are also subjected to inward buckling in the plane of the gasket. The flange surfaces prevent any out-of-plane movement of the windings and allow them to move only in the radial direction; thus inward bucking is possible in the absence of the inner ring. Figure 7 gives the inplane buckling load of metal windings subjected to a lateral pressure depending on the number of windings and whether they are welded together or not. In SW gaskets usually the first 2 to 4 windings do not contain any filler and the first 2 or 3 are spot welded together. Inward buckling is mainly resisted by these first unfilled windings. Lateral pressure is produced by the filler material that can lead to inward buckling and the results are given up to the twentieth mode. The theoretical value of the buckling pressure is about 15 MPa for mode 20, which represents about the same pressure

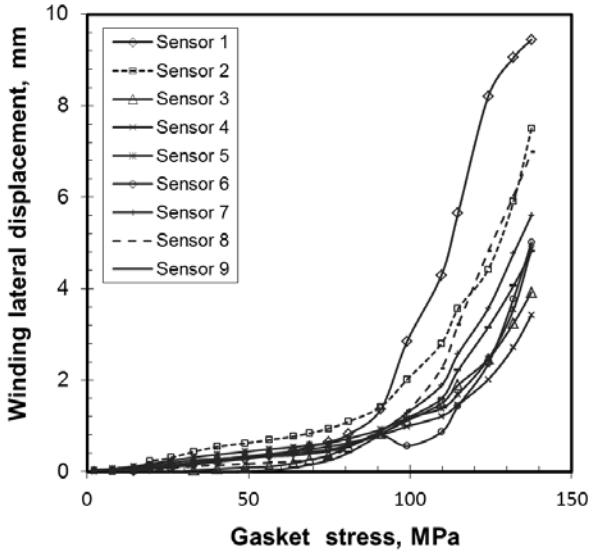

Figure 11: Winding inward radial displacement as a function of gasket compressive stress

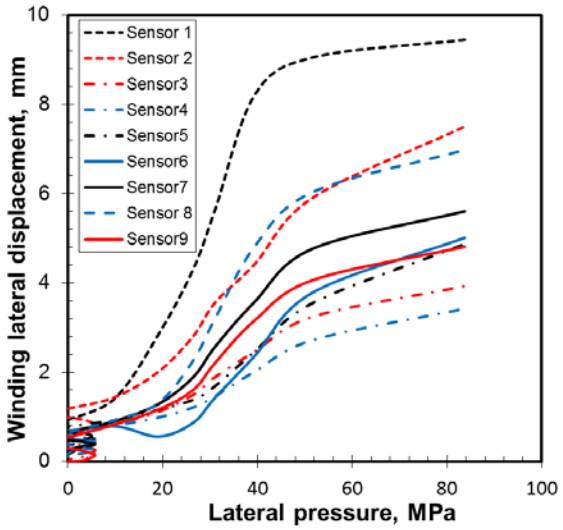

Figure 12 Winding inward radial displacement as a function of lateral pressure

obtained by the experiment shown in Fig. 11. A major increase in the inner winding movement is also reported and can be seen in Fig. 10. The difference is due to the presence of a compressive stress on the windings in the experimentation that is not considered in the analytical model, in addition to the fact that the windings are not free to deform towards the outside diameter.

Figure 8 shows the load compression curve obtained from the test which is typical to SW gasket. The curve shows that the ring was hit at 2 mm instead of 1.5 mm. This is because the LVDT is placed at the flange outside diameter picking up some flange rotation. A comparison between the numerical and experimental results is also shown in Fig. 9. The tentative FE simulation of the gasket compression was one of the model validation criteria. This was not straight forward to obtain because of the lack of the graphite mechanical properties for small strips. Nevertheless, the results show that a similar trend exists between the FE simulation and the experimental data which gives confidence on the approach used to treat the SW gasket buckling issue.

Figure 9 gives the deformation of the strain gauge placed on the outer ring as shown in Fig. 10. The deformation takes place as the compressive load is increased. Above a certain strain value the deformation changes sign and becomes negative. This change occurs at an axial displacement of 0.8 mm which corresponds to 100 micro-strains and occurs at a gasket stress of about 75 MPa.

Figure 11 provides information about the radial displacement and inward buckling of the windings. The nine beam displacement sensors can measure radial movement of the first inside winding at every 40 degrees. The winding radial displacement is small at the beginning when the gasket compression is below 75 MPa. This corresponds to the first part of the load compression curve shown in Fig. 8 which indicates the filling of the pores and the densification of the graphite filler. The displacement increases drastically above

approximately 100 MPa gasket stress. This indicates that buckling has occurred. It is difficult to evaluate the mode of buckling that had occurred. The windings are sandwiched between the two flange raised faces, the radial displacement at several positions on the circumference are blocked and hence creating points of inflexion which imposes the buckling mode. In essence this situation is beneficial since it delays inward buckling. However the torque level in any one pass during the tightening sequence has a major influence on the friction state and the buckling mode. Looking at Fig. 10, it appears that between 15 and 20 buckling waves are present. This indicates that using Eq. (11), with three first welded windings without graphite gives a lateral inplane buckling pressure of about 25 to 35 MPa.

Figure 12 shows the inward radial displacement as a function of the lateral contact pressure estimated using Eq. (12) and (13). The maximum buckling displacement reached 9.5 mm at some circular position. When this maximum is reached, it stabilizes letting the displacement increase at other circular positions. The inward buckling of the windings is shown to have taken place at a lateral pressure between 30 and 40 MPa.

CONCLUSION

The buckling of SW gaskets is a complex phenomenon to study since any of the three elements that constitute the gasket (inner ring, sealing element windings, and outer ring) may buckle. The results obtained show that the buckling model by Way is appropriate for the outer rings and the model by Teng and Lucas is more suitable for the inner windings.

The experimental results show that the buckling mode depends on the state of the friction between the windings and the raised face surface. The flange serrations create points of inflections that influence the buckling mode and therefore make the prediction difficult to obtain. Nevertheless a fairly good agreement between the calculated buckling and the experimental data is obtained if the buckling mode is known.

REFERENCES

[1] Winter Sr. J.R. and Leon G.F., 1985, "Radially Inward Buckling of Spiral Wound Gaskets," American Society of Mechanical Engineers, Pressure Vessels and Piping Division, PVP, v 98-2, p 111-116

[2] Mueller R.T., 1996, "Recent buckling experiences with spiral wound flexible graphite filled gaskets," American Society of Mechanical Engineers, Pressure Vessels and Piping Division,, PVP vol. 326, pp. 23-34, Computer Technology - 1996: Applications and Methodology

[3] Bibel G., Fath T.; Palmer W., Riedesel R. and Westlind T., 2001, "Experimental leak testing of 16-inch Class 300 RFWN flange with and without external bending moment," Welding Research Council Bulletin, n° 461, pp. 1-54.

[4] Larson R. A. and Bibel G., 2005, "Experimental and analytical evaluation of buckling forces of a spiral wound flexible gasket," ASME Pressure Vessels and Piping Division, PVP vol. 2, pp. 97-104, Proceedings of the ASME Pressure Vessels and Piping Conference 2005 - Computer Technology, PVP2005.

[5] Timoshenko, S.P., and Gere, J.M., 1961, Theory of Stability, 2nd ed., Mc Graw-Hill, New York.

[6] Wah, T., 1967, "Buckling of Thin Circular Rings under Uniform Pressure," Int. J. Solids Structures, 3, Pergamon Press ltd., pp. 967-974.

[7] Goldberg J. E. and Bogdanoff J. L., 1962, "Out-of-plane Buckling of I-section Rings," Int. Ass. Bridge Struct. Eng., 22, pp. 73-92.

[8] Thomas M. J., 1979, Inplane and Out of Plane Buckling of Thick Rings Subjected to Hydrostatic Pressure, Ph.D. Thesis, New Jersey Institute of Technology.

[9] Teng, J.G. and R.M. Lucas, 1994, "Out-of-plane Buckling of Restrained Thin Rings of General Open Section, "Journal of Engineering Mechanics, **120** (5), pp. 929-948.

[10] Boresi, A. P., 1955, "A Refinement of the Theory of Buckling of Rings Under Uniform Pressure," Journal of Applied Mechanics, **22**, pp. 95-102.

[11] Weeks G. E., 1967, Buckling of a Pressurized Toroidal Ring under Uniform External Loading, NASA Technical Note, NASA TN D-4124, National Aeronautics and Space Administration - Washington, D. C.

[12] ANSYS, 2003, Ansys Standard Manual, Version 11.0.

[13] Mathan G. and Prasad N.S., 2010, "Evaluation of Effective Material Properties of Spiral Wound Gasket through Homogenization," International Journal of Pressure Vessels and Piping, **87** (12), p 704-13

[14] Mc.Carthy J., Fitzgerald, A. and Reid D., 2013, "Spiral Wound Gasket Compressibility and Pressure Ratings," Proceedings of the ASME 2013 Pressure Vessels and Piping Conference PVP2013, July 14-18, Paris, France.

[15] Hill, R., 1950, The Mathematical Theory of Plasticity, Clarendon Press, Oxford.

[16] Mendelson, A., 1968, Plasticity: Theory and Application, The Macmillan Company, New York.

[17] Diany M. and Bouzid A., 2006, "Evaluation of Contact stress in Stuffing Box Packings," Proceedings of the 2006 ASME Pressure Vessels and Piping Division Conference, Vancouver, BC, Canada.